

Threshold anomaly in the elastic scattering of ${}^6\text{He}$ on ${}^{209}\text{Bi}$ A. R. Garcia,¹ J. Lubian,^{2,*} I. Padron,¹ P. R. S. Gomes,² T. Lacerda,² V. N. Garcia,² A. Gómez Camacho,³ and E. F. Aguilera³¹*Centro de Aplicaciones Tecnológicas y Desarrollo Nuclear (CEADEN), Playa, Ciudad de la Habana, Cuba*²*Instituto de Física, Universidade Federal Fluminense, Av. Litoranea s/n, Gragoatá, Niterói, R.J., 24210-340, Brazil*³*Departamento del Acelerador, Instituto Nacional de Investigaciones Nucleares, Apartado Postal 18-1027, C.P. 11801, México, D.F.*

(Received 31 August 2007; published 26 December 2007)

The energy dependence of the optical potential for the elastic scattering of ${}^6\text{He}$ on ${}^{209}\text{Bi}$ at near and subbarrier energies is studied. Elastic angular distributions and the reaction cross section were simultaneously fitted by performing some modifications in the ECIS code. A phenomenological optical model potential with the Woods-Saxon form was used. There are signatures that the so-called breakup threshold anomaly (BTA) is present in this system having a halo projectile ${}^6\text{He}$, as it had been found earlier for systems involving stable weakly bound nuclei.

DOI: [10.1103/PhysRevC.76.067603](https://doi.org/10.1103/PhysRevC.76.067603)

PACS number(s): 24.10.Eq, 24.10.Ht, 25.70.Bc

One of the most widely used methods for studying the interplay between different reaction mechanisms at near barrier energies is the study of the energy dependence of the optical potential. This energy dependence is produced by polarization potentials originated from the coupling between the elastic scattering and different reaction mechanisms, such as inelastic excitation, transfer of nucleons or clusters of nucleons, breakup, fusion, fission, and quasifission. These mechanisms may produce polarizations of different signs, attractive or repulsive. The net effect on the energy dependence of the total optical potential depends on the importance and strength of the different specific polarization potentials. For systems containing only tightly bound nuclei, usually the most important couplings are inelastic excitations of target and projectile and the transfer of nucleons or clusters of nucleons between them. For these systems, an attractive polarization potential is produced, and, consequently, they usually show enhancement of the fusion cross section at energies near and below the Coulomb barrier, when compared with predictions from one-dimensional barrier penetration models (or no-coupling calculations). For these systems, the energy dependence of the optical potential shows the so-called threshold anomaly (TA), which manifests itself as a decrease in the strength of the imaginary potential as the incident energy decreases toward and below the nominal Coulomb barrier. As the real and imaginary parts of the nuclear potential are connected through the dispersion relation, due to the general principle of causality [1,2], this behavior of the imaginary potential is accompanied by a bell shape of the real part of the potential, at the same energy region.

When weakly bound nuclei are involved in the interaction, the breakup channel may remain open at energies below the Coulomb barrier, with very large cross section. Then, the imaginary part of the potential does not vanish near or even below the barrier, since an important reaction channel does not close at this energy regime. Actually, for stable weakly bound nuclei, such as ${}^6,7\text{Li}$ and ${}^9\text{Be}$, it has been observed [3–5] that the strength of the imaginary part of the optical potential increases

as the energy is reduced toward the nominal Coulomb barrier. From this characteristic of the imaginary potential and because of the dispersion relation, the strength of the real part of the potential decreases at this energy region. This phenomenon is called the breakup threshold anomaly (BTA) [3]. For halo or neutron skin nuclei, not only the breakup channel but also transfer channels may remain open, with cross sections much larger than for fusion, at energies below the fusion barrier.

The aim of the present work is to investigate the presence of BTA when halo or neutron skin nuclei are involved. However, this is a very difficult task, since its manifestation should occur at energies near and below the Coulomb barrier, where the interacting potential is predominantly the Coulomb potential. For scattering of secondary beam projectiles, the situation is even worse because of the low intensities of such beams.

The approach most widely used to study the TA is to adopt the Woods-Saxon form for both real and imaginary parts of the optical potentials. However, this approach has the disadvantage of containing several free parameters in the real and imaginary parts of the potential, and consequently it leads to many ambiguities. To minimize these ambiguities, usually one calculates the potential at the strong absorption or sensitivity radius, where all the potential families have the same strength [6].

In the literature, one finds some apparent contradictions regarding the effect of the breakup of stable weakly bound nuclei on the energy dependence of the elastic scattering [4,5,7–21]. For different targets, the elastic scattering of the same stable weakly bound projectile may show the usual TA, absence of any anomaly, or the BTA. To check if these different behaviors were due to the methodologies used to study the elastic angular distributions, the systems ${}^6,7\text{Li}+{}^{27}\text{Al}$ were studied in Refs. [4,5,7] using different potentials, varying from the phenomenological with the Woods-Saxon form to the double folding and the admixture of them. The three approaches led to the same results. So, we believe that possible reasons for the different behaviors for systems with the same projectile and different targets are the competition between the Coulomb and nuclear breakups or the contribution of different multipolarities, which may be different in these various systems.

*lubian@if.uff.br

So far, the energy dependence of the optical potential in the scattering of weakly bound nuclei with halo or neutron skin structure has been scarcely studied. In the present work, we study the elastic scattering of the ${}^6\text{He}+{}^{209}\text{Bi}$ system using the phenomenological approach. The ${}^6\text{He}+{}^{209}\text{Bi}$ system has been studied before [22–24] through other approaches.

As a first step, we analyzed the elastic angular distributions for the ${}^6\text{He}+{}^{209}\text{Bi}$ system reported in Refs. [25,26] for the c.m. energies of 14.3, 15.8, 17.4, 18.6, and 21.4 MeV. The nominal Coulomb barrier for this system is approximately 20.3 MeV [25,27]. The calculations were performed using the ECIS code [28]. However, this analysis was not conclusive, since the error bars for the strength of the phenomenological potential values at the sensitivity radius were too large because of the small number of data points in the angular distributions, specially in the rainbow region, and the low statistics associated with each data point.

To overcome this problem, we included the reaction cross sections σ_R [25,26] in the fit procedure. We minimized the quantity

$$\chi^2 = \sum_{i=1}^N \left[\frac{\left(\frac{d\sigma_{\text{Elast.}}}{d\sigma_{\text{Ruth.}}} \right)^{\text{Theor.}}(\theta_i) - \left(\frac{d\sigma_{\text{Elast.}}}{d\sigma_{\text{Ruth.}}} \right)^{\text{Exp.}}(\theta_i)}{\Delta \left(\frac{d\sigma_{\text{Elast.}}}{d\sigma_{\text{Ruth.}}} \right)^{\text{Exp.}}(\theta_i)} \right]^2 + \left[\frac{\sigma_R^{\text{Theor.}} - \sigma_R^{\text{Exp.}}}{\Delta \sigma_R^{\text{Exp.}}} \right]^2, \quad (1)$$

where N is the number of data points in the elastic scattering angular distribution for a given energy.

For this purpose, some modifications were required to the original version of the ECIS code in order to minimize this quantity in the fit procedure. In the present work, reaction cross section values σ_R stand as experimental results from the direct measurement of the sum of fusion, transfer, and breakup yields; i.e., it is an independent quantity from $\frac{d\sigma_{\text{Elast.}}}{d\sigma_{\text{Ruth.}}}$. We would like to point out that reaction cross sections are usually deduced values of cross sections obtained when one fits elastic angular distributions in a one-channel calculation (optical model calculations). This may be a good approximation when the number of points in the angular distribution is much larger than the ones available for this system, but not in the present situation.

The approach applied to minimize the quantity given in Eq. (1) was to use Woods-Saxon form factors for both real and imaginary parts of the nuclear optical potential. Contrary to what was done in Refs. [22–24], we do not divide the direct and compound contributions in the absorption potential but rather consider the total absorption of flux, since our present interest is to verify the possible presence of the BTA in the elastic scattering of this system. The radii for the real and imaginary potentials were fixed at $R_V = R_W = 9.68$ fm to minimize the ambiguities in the fitting procedure. These values correspond to the sum of the root mean square radii of the projectile and target. The depths and diffuseness V , W , a_V , and a_W were kept as free parameters in the fitting procedure. The starting values for V and a_V were taken as the ones used in the study of the elastic scattering of ${}^4\text{He}$ on ${}^{209}\text{Bi}$ at 22.0 MeV [29]. As for the imaginary part parameters, W and a_W , the ones used in

TABLE I. Optical potential parameters and σ_R for each energy.

$E_{\text{c.m.}}$ (MeV)	V (MeV)	a_V (fm)	W (MeV)	a_W (fm)	χ^2	$\sigma_R^{\text{Exp.}}$ (mb)	$\sigma_R^{\text{Theor.}}$ (mb)
14.3	127.2	0.90	24.0	1.29	28.3	189(27)	215.0
15.8	130.0	0.73	19.0	1.21	7.0	302(32)	318.0
17.3	132.2	0.63	10.6	1.31	3.5	585(40)	572.4
18.6	134.6	0.44	8.0	1.33	7.7	716(59)	708.7
21.4	137.1	0.49	15.0	1.03	14.1	1083(54)	1088.6

the elastic scattering of ${}^6\text{He}$ on ${}^{208}\text{Pb}$ at 27.0 MeV [30] were adopted.

Table I shows the optical model parameters that lead to the best fit of the angular distributions. χ^2 values correspond to the quantity given in Eq. (1). It is important to notice that the values of the diffuseness of the imaginary potential are systematically larger than the ones of the real potential and that their values are also much larger than the usual values of 0.65 fm. This shows that the absorption of flux from the elastic channel starts to occur at long distances, as it should be expected for projectiles with halo structure, for which it has already been shown that polarization potentials have a long tail due to the presence of the breakup channel [31,32]. The last two columns of Table I show the experimental and the best fit values for the reaction cross sections. Figure 1 shows

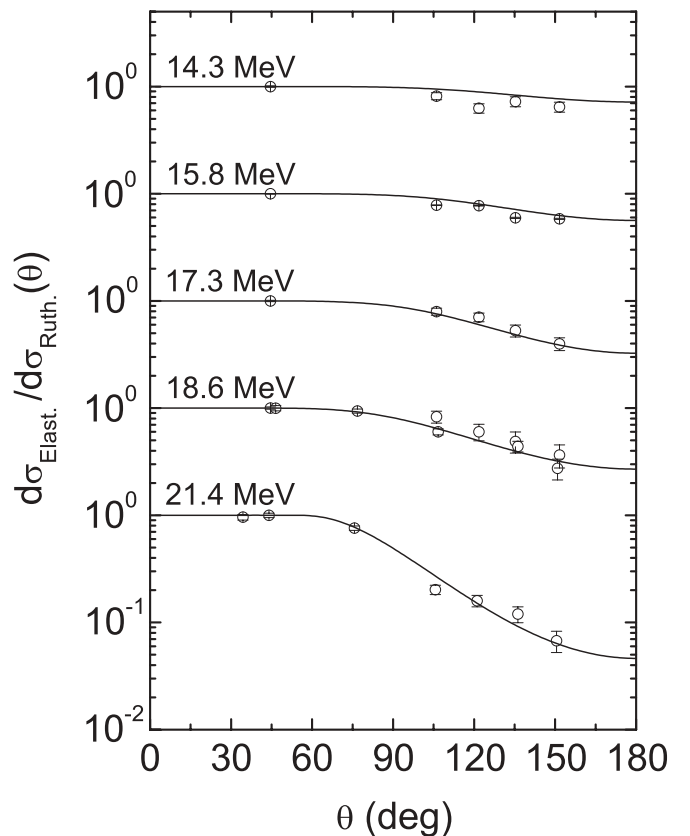


FIG. 1. Elastic scattering angular distributions for the different energies studied. Curves are obtained from calculations described in the text.

the fit to the elastic angular distributions. One can see that the fits are quite good in the whole energy range, except for the elastic angular distribution at the lowest energy, where there is some overestimation of the data. A reasonable fit of the elastic scattering angular distribution at the lowest energy at $E_{c.m.} = 14.3$ MeV has not been achieved by any of the previously reported attempts to do so [22,24,25,33]. The reason for that might be some normalization problem with data, the intrinsic difficulty at such low energy, or the lack of transfer channels in the coupling scheme (as will be explained later in this paper). Even so, we kept the data for this energy in our analysis. For $E_{c.m.} = 18.6$ MeV, there were two sets of data, as can be observed in Fig. 1. In the fit procedure, obviously the dataset with smaller error bars, corresponding to the smaller cross sections, has a larger weight. The fit for this dataset is good. To obtain the sensitivity radii for the real and imaginary parts of the optical potential, first the diffuseness parameters of the real part were varied in steps of $\Delta a_V = 0.02$ fm, and the depths were fitted again. The same procedure was repeated for the imaginary part of the optical potential. This procedure allowed us to obtain the crossing point of different families of the optical potential, i.e., the so-called radius of sensitivity. These radii are very slowly energy dependent. The mean value for the sensitivity radius is $R_S = 14.59$ fm for both real and imaginary parts of the potential.

Figure 2 shows the energy dependence of the real (upper panel) and imaginary (lower panel) parts of the optical potential at the sensitivity radius. The error bars correspond to

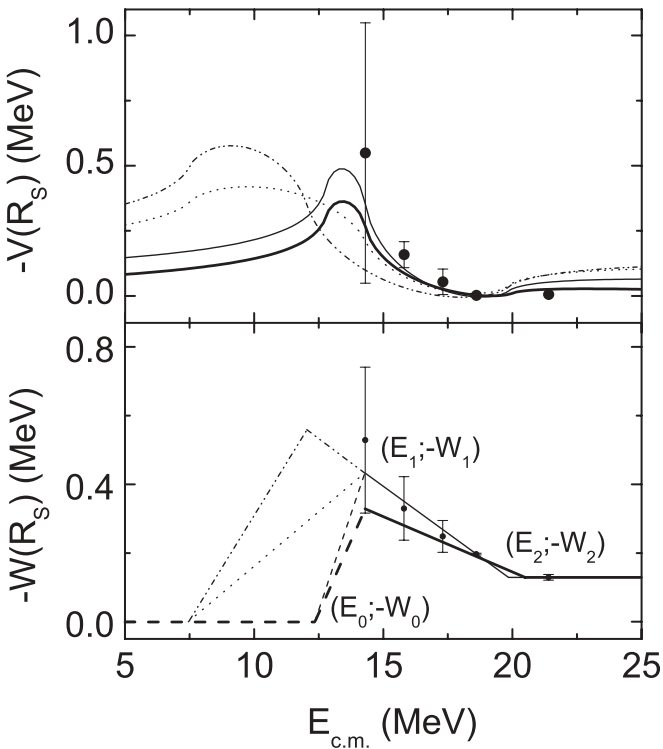


FIG. 2. Energy dependence of the real (upper panel) and imaginary (lower panel) parts of the optical potential at the sensitivity radius (see text for details).

the variation of the $\frac{\chi^2}{N+1}$ in one unit, where N is the number of data points of the elastic angular distributions for a given energy. In the lower panel, the thick solid and dashed lines represent a schematic behavior for the imaginary part of the optical potential given by the parametrization

$$W(E) = \begin{cases} 0 & E \leq 12.8 \\ 0.65W_1(E - 12.8) & 12.8 \leq E \leq 14.3 \\ W_1 + \left(\frac{W_1 - W_2}{E_2 - 14.3}\right) & 14.3 \leq E \leq E_2 \\ W_2 & E \geq E_2 \end{cases}, \quad (2)$$

where the energies are given in MeV and the ordered pairs $(E_0 = 12.8$ MeV, $W_0 = 0)$, $(E_1 = 14.3$ MeV, $W_1 = -0.43$ MeV), and $(E_2 = 19.6$ MeV, $W_2 = -0.13$ MeV) are shown in Fig. 2. The dashed curve at low energies corresponds to one of the several possibilities for the behavior of the imaginary potential at this energy regime and is not supported by experimental data. The only thing that we can say is that below a certain energy, the total reaction cross section must vanish and so does the imaginary potential. In this parametrization, E_0 is the energy for which the reaction cross section vanishes. E_1 is the value from which the imaginary potential starts to drop to zero, as the energy decreases. E_2 is the value above which the imaginary potential is energy independent. The choice of E_0 was governed by the extrapolation of the empirical expression $\sigma_R(E) = 128.1E - 166.8$ mb given in Ref. [25]. The choice of the value of E_1 is arbitrary, but our conclusions do not depend on this choice. Only the shape of the real part is slightly modified by the variation of the value of E_1 . The thick solid line in the upper panel of Fig. 2 corresponds to the dispersion relation calculation using the schematic segment representation of $W(E)$ given in Eq. (2). In Fig. 2 we show, as dotted and dotted-dashed curves, two other possible parametrizations for the imaginary potentials and the corresponding real potentials. The dotted curve is not so sharp, a behavior more compatible with calculations performed by Keeley and Mackintosh [34] for the ${}^6\text{He} + {}^{208}\text{Pb}$ system, in which the long-range breakup induced potentials do not vary too much at subbarrier energies. For the dotted-dashed curves, the energy for which the imaginary potential starts to decrease is smaller than in the first parametrization. Finally, the thin solid and dashed curves correspond to a parametrization which fits the real potential at the highest energy. One can notice that although the real and imaginary parts of the potential have different forms in each parametrization, our conclusion about the presence of the BTA will not change.

From the points in Fig. 2, one may observe a clear increasing trend of the imaginary potential strength for the four lowest energies, all of them at the subbarrier energy region, when the energy decreases from E_2 to E_1 . However, one could argue that the lowest energy has such a large error bar and such a bad fit of the angular distribution (see Fig. 1), that it could not be used to confirm the BTA phenomenon for this system. If one wants to be even more cautious, one might say that at $E_{c.m.} = 18.6$ MeV, the strength of the imaginary potential is roughly the same as for the highest energy. Even so, points

at two other energies show a clearly increasing trend of the imaginary potential as the energy decreases. So far, BTA has not been observed for more than two energies, even when stable beams were involved and much more precise angular distributions were available: ${}^6\text{Li}+{}^{208}\text{Pb}$ [3] and ${}^6\text{Li}+{}^{27}\text{Al}$ [5]. For the other three systems, BTA has been suggested to occur based in the behavior of the imaginary potential at only one energy [35]. So, we believe that the signatures of the presence of BTA for this system are compatible with the ones observed for stable beams.

A very important point to mention is that although the behavior of the real and imaginary polarization potentials is exactly the typical one of the BTA phenomenon, in this situation where the projectile is ${}^6\text{He}$, one should be careful before saying that the observed behavior is exclusively due to the coupling to the breakup channel. The reason for that comes from experimental evidence that the transfer of one or two neutrons have very large cross sections for the similar ${}^6\text{He}+{}^{238}\text{U}$, ${}^{208}\text{Pb}$ systems [36,37], even at energies below

the Coulomb barrier. For the ${}^6\text{He}+{}^{209}\text{Bi}$ system, experiments [38,39] show that one and two neutron transfer channels have large cross sections above the Coulomb barrier. However, for this system, four-body continuum discretized coupled channel (CDCC) calculations for energies above the barrier, performed by T. Matsumoto *et al.* [32], show that at this energy regime, there is no room for transfer reactions as important coupling channels, because when only the coupling to the breakup channel is included in the calculations, there is good agreement with data for the elastic angular distributions. So, as mentioned earlier in this paper, transfer channels may explain the failure of our calculations to reproduce the elastic scattering angular distribution at the low energy of 14.3 MeV. So, one open question is whether this apparent BTA is due to the breakup itself or it is also influenced by transfer channels at subbarrier energies. This aspect needs to be further investigated.

The authors acknowledge the financial support from CNPq and FAPERJ.

-
- [1] G. R. Satchler, Phys. Rep. **199**, 147 (1991).
 [2] M. A. Nagarajan, C. C. Mahaux, and G. R. Satchler, Phys. Rev. Lett. **54**, 1136 (1985).
 [3] M. S. Hussein, P. R. S. Gomes, J. Lubian, and L. C. Chamon, Phys. Rev. C **73**, 044610 (2006); **76**, 019902(E) (2007).
 [4] J. O. Fernández Niello *et al.*, Nucl. Phys. A **787**, 484c (2007).
 [5] J. M. Figueira *et al.*, Phys. Rev. C **75**, 017602 (2007).
 [6] M. E. Brandan *et al.*, Phys. Rev. C **48**, 1147 (1993).
 [7] J. M. Figueira *et al.*, Phys. Rev. C **73**, 054603 (2006).
 [8] J. Lubian *et al.*, Nucl. Phys. A **791**, 24 (2007).
 [9] L. F. Canto, P. R. S. Gomes, R. Donangelo, and M. S. Hussein, Phys. Rep. **424**, 1 (2006).
 [10] N. Keeley *et al.*, Nucl. Phys. A **571**, 326 (1994).
 [11] A. M. M. Maciel *et al.*, Phys. Rev. C **59**, 2103 (1999).
 [12] S. B. Moraes *et al.*, Phys. Rev. C **61**, 064608 (2000).
 [13] K. Rusek and K. W. Kemper, Phys. Rev. C **61**, 034608 (2000).
 [14] J. Lubian *et al.*, Phys. Rev. C **64**, 027601 (2001).
 [15] A. Pakou *et al.*, Phys. Lett. B **556**, 21 (2003).
 [16] A. Pakou *et al.*, Phys. Rev. C **69**, 054602 (2004).
 [17] R. J. Woolliscroft *et al.*, Phys. Rev. C **69**, 044612 (2004).
 [18] P. R. S. Gomes *et al.*, Phys. Rev. C **70**, 054605 (2004).
 [19] P. R. S. Gomes *et al.*, Phys. Rev. C **71**, 034608 (2005).
 [20] P. R. S. Gomes *et al.*, Rev. Mex. Fís. **S52**, 23 (2006).
 [21] P. R. S. Gomes, I. Padron, and J. Lubian, J. Radiol. Nucl. Chem. **272**, 215 (2007).
 [22] B. T. Kim, W. Y. So, S. W. Hong, and T. Udagawa, Phys. Rev. C **65**, 044616 (2002).
 [23] A. Gómez Camacho *et al.*, Phys. Rev. C **76**, 044609 (2007).
 [24] A. Gómez Camacho and E. F. Aguilera, Rev. Mex. Fís. **50**, 265 (2004).
 [25] E. F. Aguilera *et al.*, Phys. Rev. C **63**, 061603(R) (2001).
 [26] E. F. Aguilera *et al.*, Phys. Rev. Lett. **84**, 5058 (2000).
 [27] J. J. Kolata *et al.*, Phys. Rev. Lett. **81**, 4580 (1998).
 [28] J. Raynal, in *Proceedings of the Workshop on Applied Nuclear Theory and Nuclear Model Calculations for Nuclear Technology Applications, Trieste*, edited by M. K. Mehta and J. J. Schmidt (World Scientific, Singapore, 1989), p. 506.
 [29] A. R. Barnett and J. S. Lilley, Phys. Rev. C **9**, 2010 (1974).
 [30] O. R. Kakuee *et al.*, Nucl. Phys. A **765**, 294 (2006).
 [31] J. Lubian and F. M. Nunes, J. Phys. G: Nucl. Part. Phys. **34**, 513 (2007).
 [32] T. Matsumoto *et al.*, Phys. Rev. C **73**, 051602(R) (2006).
 [33] J. J. Kolata, Eur. Phys. J. A **13**, 117 (2002).
 [34] N. Keeley and R. S. Mackintosh, Phys. Rev. C **71**, 057601 (2005).
 [35] P. R. S. Gomes *et al.*, J. Phys. G **31**, S1669 (2005).
 [36] R. Raabe *et al.*, Nature (London) **431**, 823 (2004).
 [37] D. Escrib *et al.*, Nucl. Phys. A **792**, 2 (2007).
 [38] P. A. DeYoung *et al.*, Phys. Rev. C **71**, 051601(R) (2005).
 [39] J. P. Bychowski *et al.*, Phys. Lett. B **596**, 26 (2004).